Deep-learning based automatic segmentation of vesicles in cryo-electron tomograms

Authors

- **Amin Khosrozadeh**[*]
  [XXXX-XXXX-XXXX-XXXX](#) · [ameen-khosrowzadeh](#)
  Institute of Anatomy, University of Bern, Bern, Switzerland; Graduate School for Cellular and Biomedical Sciences, University of Bern · Funded by Grant XXXXXXXX

- **Raphaela Seeger**[*]
  [XXXX-XXXX-XXXX-XXXX](#) · [elatella](#)
  Institute of Anatomy, University of Bern, Bern, Switzerland; Graduate School for Cellular and Biomedical Sciences, University of Bern

- **Julika Radecke**
  [0000-0002-5815-5537](#) · [julikaradecke](#)
  Institute of Anatomy, University of Bern, Bern, Switzerland; Department of Neuroscience, Faculty of Health and Medical Science , 2200 Copenhagen N, University of Copenhagen, Copenhagen, Denmark; Diamond Light Source Ltd, Didcot, Oxfordshire, United Kingdom

- **Guillaume Witz**
  [0000-0003-1562-4265](#) · [guiwitz](#)
  Science IT Service, University of Bern, Bern, Switzerland

- **Vladan Lučić**
  [0000-0003-3698-7436](#) · [vladanl](#)
  Max-Planck-Institute of Biochemistry, Am Klopferspitz 18, 82152 Martinsried, Germany

- **Jakob B. Sørensen**
  [0000-0001-5465-3769](#) · [JBSorensen](#)
  Department of Neuroscience, University of Copenhagen, Blegdamsvej 3B, 2200 Copenhagen N, Denmark · Funded by Novo Nordisk Fonden, NNF17OC0028516.; Carlsbergfondet, CF17-0875; Independent Research Fond Denmark, 8020-00228A; Lundbeckfonden, R277-2018-802

- **Benoît Zuber**[✉]
  [0000-0001-7725-5579](#) · [aseedb](#)
  Institute of Anatomy, University of Bern, Bern, Switzerland · Funded by Swiss National Science Foundation, 179520; ERA-NET NEURON, NEURON-119

✉ — Address correspondence to benoit.zuber@ana.unibe.ch.

* These authors contributed equally.

Abstract

The communication between neurons is based on the exocytosis of neurotransmitter filled vesicles. Even small disbalances in this delicate system can result in different disorders. Numerous questions are still unanswered about synaptic vesicle exocytosis regulation as well as about which proteins affect this fundamental process. Hundreds to thousands of vesicles are present at the synapse and most of them are interconnected. There is a number of evidence suggesting that the connectivity between the vesicles influences synaptic vesicle exocytotic activity and that connectivity can be regulated. To address these issues, cryo-electron tomography is a method of choice. Yet inevitable quantitative studies require accurate segmentation of both synaptic vesicles and the interconnecting filaments.

This segmentation process has been widely recognized as a bottleneck by the community. When working with synapses, an incredibly tedious cellular feature to segment are synaptic vesicles. Even though they have a very homogeneous shape and size, which makes it easy to distinguish them from other cellular features, their high occurrence makes their segmentation challenging (one average-sized synapse or synaptosomes can easily contain between 300-500 synaptic vesicles).

Several attempts at utilizing machine learning algorithms to automize the segmentation of synaptic vesicles yielded in unfavorable results. We analyzed these approaches and realized that most algorithms solely worked with the 2D image planes within the tomogram, but didn't tap into their 3D information and therefore increased the weight of the missing wedge.

We designed a framework that consists of two parts: 1) U-Net convolutional network to obtain mask for SVs following by 2) post-processing step which fine-tunes the mask and provides entire 3D-vesicles. A deep-learning model has been trained with manually segmented synaptic vesicles, which have been entirely annotated as 3D objects. By post-processing, we achieved to transfer the vesicle recognition through this pipeline. The evaluation metrics like the DICE value suggest a very high success rate.

Introduction

The rise of machine learning is sweeping the technological landscape.

While machine learning has been around for several decades prior to its boom, and it theoratically would be able to learn anything using a shallow neural network of 1 hidden layer (universal approximation theorem by Cybenko), more complex problems required several hidden layers. However, with an increased number of hidden layers, the chance of finding the correct weights, which are initialized as random numbers, through backpropagation is low, as they are being multiplied over the layers and eventually approach 0. The initilizing booster for this hype in 2006 was moving from back propagation in multiple layer neural networks and eventually vanish (they are fractions) to deep learning [1]. Deep learning uses a new initalization strategy: series of single layer networks. (check the prior 2 sentences, especially if the citation fits) In the following years many new publications revolutinized the field further with new concepts of how to train deep neural networks [**doi:10.5555/3042817.3043064?**]

Since then the use cases of deep learning have become highly diverse and are just starting to reach the scientific community. Especially the graphical deep-learning approaches have been quite popular [2]. Its approach is based around learning the description of the common attributes of a group or subset of a universe of objects [3]. The segmentation of an input image is a typical area of application. Here the computer seperates the image into different partitions, each of them representing a

different feature and traces the detected feature in the original image. Adapting this image segmentation into the medical and biological research has resulted in the design of UNet [4]. UNet is able to localise, distinguish and trace borders, by treating the segmentation as a multiclass classification problem for each pixel. Its architecture consists of two parts: the contracting part which captures context, and the symmetric expanding path that enables precise localization [5]. `*_What UNet type are we using: Extended 3D U-Net, Joint 2D-3D CNN, CNN with optimization module or Hierarchical networks_*`

But also the field of cryo electron microscopy has recently recognized the benefits of machine/deep-learning approaches [6].

The method of cryo-electron tomography (ET) utilises a series of tilted two-dimensional (2D) images to reconstruct a three-dimensional (3D) volume of the imaged sample [7].

-> Describe more about cryo EM and cryo ET, also mention missing wedge problem

It brings many advantages compared to other cryo-electron microscopy (EM) methods, as it yields images at in situ conditions. Therefore cryo ET can help to reveal the natural cellular environment of protein(-complexes), their function as well as their structure. In order to analyze the cellular context within a tomogram, cellular features are being segmented. Popular programs for manual segementation are IMOD and Amira [8,9]. Currently manual segmentation is being considered the bottleneck in the worklow timewise of cellular cryo-ET.

Our lab researches, with the help of cryo-ET, the synaptic architecture and its changes upon neurotransmitter vesicle release. A special focus in that research holds the SNARE complex, which connects the synaptic vesicles and the presynaptic cell membrane, mediating vesicle fusion. Their function and regulation still pose big questions. In addition, mutations of involved proteins have been linked to numerous neurological diseases. To address these issues, cryo-ET is the methode of choice. To perform quantitative studies on the resulting tomograms, accurate segmentation of both synaptic vesicles and the interconnecting filaments are required. Among the different cell features, synaptic vesicles are the most time consuming to segment. Despite their very homogeneous size and shape, their sheer number and finding their true center (due to the missing wedge problem) complicates their segmentation.

Problem 2D and 3D

Our aim is the creation of a deep-learning pipeline, which is taught to segment cellular features, starting with synaptic vesicles. We decided to teach our network with a real world dataset rather than using synthetic datasets, as it is often custom, as the synthetic datasets lack noise and would represent a complete 360° 3D object, which our datasets cannot due to the missing wedge problem in cryo-ET. Our proposed method provides the initial step for downstream segmentation of subcellular compartments such as synaptic connectors and tethers for which an extremely accurate vesicle segmentation is required.

Results

Comparison of manual segmentation with automatic deep-learning based segmentation

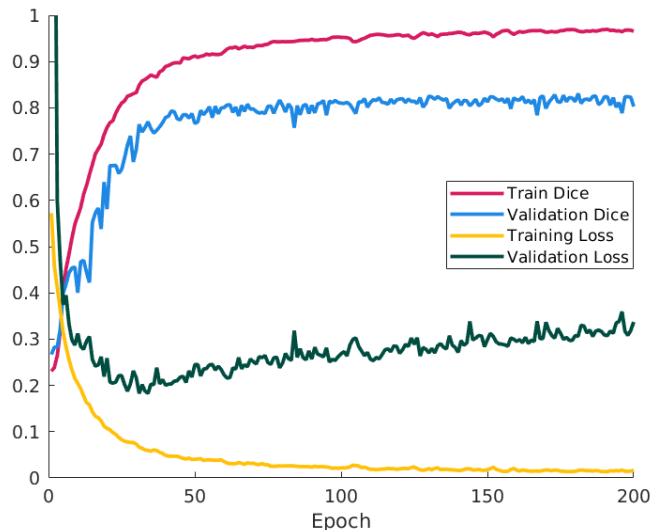Evaluation metric DICE for pixel/pixel analysis Global analysis

Figure 1: Dice coefficient and loss value for training and validation set.

3d unet good for 3D processing recent Nature methods paper by Ben Engel, DeepFinder -> Relion for STA creates mask to find more using dl -what are they doing, maybe compare that in the text, different aims; we might compare results we achieve (keep as bonus, revision)

3 different types of dl: classification, localization and segmentation We specialize in accurity segmenting 3D svs -> results through the network, output is a mask, smooth DICE/ binary DICE = which one for our mask? one function for both? -> Amin will check when we encounter error until now we remove sv(?), bug inside function -> fix bug for better performance, how many fail and why? evaluation: objectwise evaluation for I/O, radius, center (according to nature paper) -> compare with manual seg other common evaluation tool other than DICE (Amin wants to check)

Discussion

DICE

Outlook

implement automatic cell-outline and active zone segmentation as deep learning workflow using UNet implement automatic connector and tether segmentation as a deep leaning workflow using UNet

Materials and methods

Cryo-electron Tomography Datasets

Two datasets of different origin were used as input and test subjects for the automatic segmentation pipeline, rat synaptosomes as well as astrocytic and neural cell cultures derived from mice. `\_cite Vladan, segmentation write a bit more*`

Rat synaptosomes

The preparation of the rat synaptosomes were previously described [10]. After the purification, the synaptosomes were incubated for 30min at room temperature. 1.3mM CaCl2 and 10 nm gold fiducials were added (gold fiducials, #s10110/8. AURION Immuno Gold Reagents & Accessories. Wageningen,

The Neatherlands). The synaptosome solution was applied to a 200-mesh lacey finder carbon film grid (#AGS166-H2. Agar Scientific. Elektron Technology UK Ltd. Stansted, UK). Manual blotting was used to remove exess liquid with the aid of a filter paper. Thereafter the grid was immediately plunge frozen in liquid ethane using a homebuilt plunge freezer controlled with a LabView script (National Onstruments Corporation. Mopac Expwy Austin, TX, USA). The grids coated with rat synaptosomes were mounted in a cryo-holder (Gatan, Pleasonton, CA, USA) and transferred to a Tecnai F20 (FEI, Eindhoven, The Netherlands) which was set to low dose conditions, operated at 200 kV, and equipped with a field emission gun. Images were recorded with a 2k x 2k CCD camera (Gatan) mounted after a GIF Tridiem post-column filter (Gatan) operated in zero-loss mode. The sample was kept at about -180°C. Tilt series were acquired using SerialEM [11] for automated acquisition recorded typically from -50° to 50° with a 2° angular increment and an unbinned pixel size of 0.75 or 1.2 nm. Due to sample thickness (400-700 nm), tomograms were usually not recorded with higher tilt angles. Defocus was set between -8 to -12 μm and the total electron dose used was about 80-100 $e^-/Å^2$. Some tomograms were acquired at a Titan Krios equipped with a K2 direct electron detector (Gatan) without energy filter. The K2 camera was operated in superresolution counting mode and between 8-40 frames per tilt angle were taken. Tilt series were acquired using the Latitude software (Gatan) for automated acquisition recorded typically from -60° to 60° with a 2° angular increment and an unbinned pixel size of 0.6 nm. Defocus was set between -8 to -12 μm and the total electron dose used was about 80-100 $e^-/Å^2$. Prior to image processing the frames at each tilt angle, frames were aligned and averaged in 2dx MC_Automator [12] with motioncor [13]. 3D reconstruction was done in IMOD [8]. The alignments were done using the automated fiducial tracking function and the 3D reconstructions were done using the weighted back projection followed by a nonlinear anisotropic diffusion (NAD) filtering.

Astrocytic and neuronal mouse culture

The preparation of astrocytic and neuronal culture has been published before [14]. After 12 to 14 days of incubation grids with mouse neurons were plunge frozen with a Vitrobot (Thermofisher Scientific, Mark IV) with a blot time of 3 s and a blot force of -10. Wait time and drain time were not used. Humidity was set to 100% at 4°C. 4 undiluteted 10 nm BSA gold tracer (Aurion) was added directly onto the grid prior to plunge freezing. Cultured mouse neurons tilt series were acquired at a Titan Krios, equipped with a Falcon 3 direct electron detector (Thermofisher Scientific) without energy filter. The Falcon camera was operated in linear mode. Tilt series were acquired using the TEM Tomography software (TFS) for automated acquisition recorded typically from -60° to 60° with a 2° angular increment and an unbinned pixel size of 0.37 nm. Defocus was set between -6 to -10 μm and the total electron dose used was about 80-100 $e^-/Å^2$. Tomogram reconstruction was done in the same way as for the synaptosome datasets.

Manual segmentation procedures

Manual segmentation of SVs, mitochondria, and the active zone PM was done in IMOD (Figure S4A&B). The boundary marked the region to be analyzed by Pyto [15]. The analysis by Pyto was essentially the same as described previously [16] [15].

In short, the segmented area is divided in 1 voxel thick layers parallel to the active zone for distance calculations. A hierarchical connectivity segmentation detects densities interconnecting vesicles (so called connectors) and densities connecting vesicles to the active zone PM (so called tethers) (Figure S4C). Distance calculations are done with the center of the vesicle. Mainly default settings were used. The segmentation procedure is conservative and tends to miss some tethers and connectors because of noise. Consequently, the numbers of tethers and connectors should not be considered as absolute values but rather to compare experimental groups. As it was done before, an upper limit was set between 2100 and 3200 nm3 on segment volume. The tomograms that were used for this analysis were binned by a factor of 2 to 3, resulting in voxel sizes between 2.1 and 2.4 nm.

Pre-processing of manual segmentation outputs from IMOD for further use (jupyter notebook pre-pyto)

Description of Machine Learning: Training Stage

Deep Model Training

Unet Training Datasets and Batch Generation

Transfer Learning

Optimization / Postprocessing

-Global Threshold

-Mask Tuning

-Compute Radial Profile

-Radius Estimation (Cross Correlation through Radial Profile) -Remove Outlier Labels

Analysis of Results

References

1. **Reducing the Dimensionality of Data with Neural Networks**
   GE Hinton, RR Salakhutdinov
   Science (2006-07-28) https://doi.org/b7vgmj
   DOI: 10.1126/science.1127647 · PMID: 16873662

2. **Machine Learning in Medicine**
   Alvin Rajkomar, Jeffrey Dean, Isaac Kohane
   New England Journal of Medicine (2019-04-04) https://doi.org/gfzk8r
   DOI: 10.1056/nejmra1814259 · PMID: 30943338

3. **A review of machine learning**
   David M Dutton, Gerard V Conroy
   The Knowledge Engineering Review (1997-12) https://doi.org/dcswnd
   DOI: 10.1017/s026988899700101x

4. **U-Net: Convolutional Networks for Biomedical Image Segmentation**
   Olaf Ronneberger, Philipp Fischer, Thomas Brox
   Medical Image Computing and Computer-Assisted Intervention – MICCAI 2015 (2015)
   https://doi.org/gcgk7j
   DOI: 10.1007/978-3-319-24574-4_28 · ISBN: 9783319245737

5. **Image Segmentation Using Deep Learning: A Survey**
   Shervin Minaee, Yuri Y Boykov, Fatih Porikli, Antonio J Plaza, Nasser Kehtarnavaz, Demetri Terzopoulos
   IEEE Transactions on Pattern Analysis and Machine Intelligence (2021) https://doi.org/gjh26c
   DOI: 10.1109/tpami.2021.3059968 · PMID: 33596172

6. **Application of machine learning techniques to electron microscopic/spectroscopic image data analysis**
   Shunsuke Muto, Motoki Shiga
   Microscopy (2020-04-08) https://doi.org/ggckm4
   DOI: 10.1093/jmicro/dfz036 · PMID: 31682260 · PMCID: PMC7141894

7. **Current data processing strategies for cryo-electron tomography and subtomogram averaging**
   Euan Pyle, Giulia Zanetti
   Biochemical Journal (2021-05-28) https://doi.org/gkqqv6
   DOI: 10.1042/bcj20200715 · PMID: 34003255 · PMCID: PMC8133831

8. **Computer Visualization of Three-Dimensional Image Data Using IMOD**
   James R Kremer, David N Mastronarde, JRichard McIntosh
   Journal of Structural Biology (1996-01) https://doi.org/d9nfzw
   DOI: 10.1006/jsbi.1996.0013 · PMID: 8742726

9. **amira: A Highly Interactive System for Visual Data Analysis**
   Detlev Stalling, Malte Westerhoff, Hans-Christian Hege
   Visualization Handbook (2005) https://doi.org/dj723z
   DOI: 10.1016/b978-012387582-2/50040-x · ISBN: 9780123875822

10. **A rapid Percoll gradient procedure for preparation of synaptosomes**
    Peter R Dunkley, Paula E Jarvie, Phillip J Robinson
    Nature Protocols (2008-11) https://doi.org/b7zwh8

DOI: 10.1038/nprot.2008.171 · PMID: 18927557

11. **Automated electron microscope tomography using robust prediction of specimen movements**
David N Mastronarde
Journal of Structural Biology (2005-10) https://doi.org/ff7gzx
DOI: 10.1016/j.jsb.2005.07.007 · PMID: 16182563

12. **2dx_automator: Implementation of a semiautomatic high-throughput high-resolution cryo-electron crystallography pipeline**
Sebastian Scherer, Julia Kowal, Mohamed Chami, Venkata Dandey, Marcel Arheit, Philippe Ringler, Henning Stahlberg
Journal of Structural Biology (2014-05) https://doi.org/f522h3
DOI: 10.1016/j.jsb.2014.03.016 · PMID: 24680783

13. **Electron counting and beam-induced motion correction enable near-atomic-resolution single-particle cryo-EM**
Xueming Li, Paul Mooney, Shawn Zheng, Christopher R Booth, Michael B Braunfeld, Sander Gubbens, David A Agard, Yifan Cheng
Nature Methods (2013-06) https://doi.org/f4zpjf
DOI: 10.1038/nmeth.2472 · PMID: 23644547 · PMCID: PMC3684049

14. **Preparation of Primary Neurons for Visualizing Neurites in a Frozen-hydrated State Using Cryo-Electron Tomography**
Sarah H Shahmoradian, Mauricio R Galiano, Chengbiao Wu, Shurui Chen, Matthew N Rasband, William C Mobley, Wah Chiu
Journal of Visualized Experiments (2014-02-12) https://doi.org/gmh9w3
DOI: 10.3791/50783 · PMID: 24561719 · PMCID: PMC4089403

15. **Hierarchical detection and analysis of macromolecular complexes in cryo-electron tomograms using Pyto software**
Vladan Lučić, Rubén Fernández-Busnadiego, Ulrike Laugks, Wolfgang Baumeister
Journal of Structural Biology (2016-12) https://doi.org/f9d5t2
DOI: 10.1016/j.jsb.2016.10.004 · PMID: 27742578

16. **Quantitative analysis of the native presynaptic cytomatrix by cryoelectron tomography**
Rubén Fernández-Busnadiego, Benoît Zuber, Ulrike Elisabeth Maurer, Marek Cyrklaff, Wolfgang Baumeister, Vladan Lučić
Journal of Cell Biology (2010-01-11) https://doi.org/b9c26b
DOI: 10.1083/jcb.200908082 · PMID: 20065095 · PMCID: PMC2812849